SLAC-PUB-5743
February 1992
(A)

SIMULATION OF TAIL DISTRIBUTIONS IN ELECTRON-POSITRON CIRCULAR COLLIDERS*

John Irwin
Stanford Linear Accelerator Center
Stanford Unioversity, Stanford, California 94309

Abstract

In addition to the Gaussian shaped core region, particle bunches in electron-positron circular colliders have a rarefied halo region of importance in determining beam lifetimes and backgrounds in particle detectors. A method is described which allows simulation of halo particle distributions.

Introduction

Although it is a simplification, one can divide the beam-beam problem into the two different regimes of core particles and halo particles. The core particles are those in the high density part of the beam, and the distribution of these particles determines the luminosity. Although improvements are still needed, many workers [3,5] have successfully modeled these particles and calculated the luminosity under real accelerator conditions.

The halo particles are a different story. While they don't determine the luminosity, they do determine the beam lifetime and the experimental backgrounds. These are as important as the luminosity because the machine must operate in a region of parameters with good lifetime and low backgrounds. In Figures 1 and 2 we show some experimental measurements of vertical tail distributions. Typically the distributions fall off exponentially rather than maintaining the Gaussian distribution which characterizes the core particles. We describe here techniques to model these halo particles.

The measurements of Figure 1 were performed by inserting a beryllium finger into the tail region. The gamma radiation resulting from bremstrahlung in the finger will be proportional to the density of particles in the beam. In principle, since cross sections and geometry are known, this could be a direct measure of the particle density. The finger must be made thick enough to be mechanically stable, yet thin enough so that the scattering in the finger does not significantly alter the particle distribution. Our estimates indicate that the scattering from the finger used by Decker and Talman would substantially alter the tail distribution.

The measurements in Figure 2 are made by inserting a scraper into the beam and observing the resulting change in beam lifetime. For typical beam currents the image fields from the scraper are strong enough to change the orbit and tune of the beam. This effect was noted and measured by the author and S. Milton. Recently S. Milton [4] has measured tail distributions for weak beams. Despite the fact that for usual operating conditions the effects of the scraper on the beam are neglected, one suspects they give a qualitative understanding of the situation.

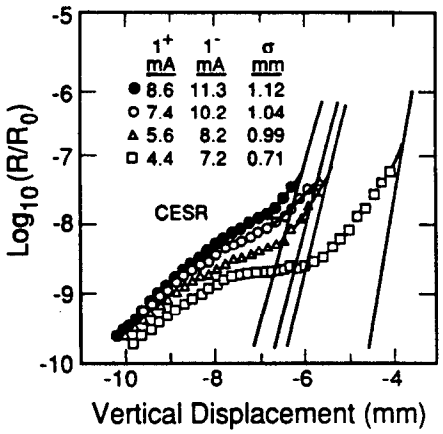

FIG. 1. Observed beam-beam produced non-Gaussian vertical beam tails using a beryllium probe in CESR as a function of current [1].

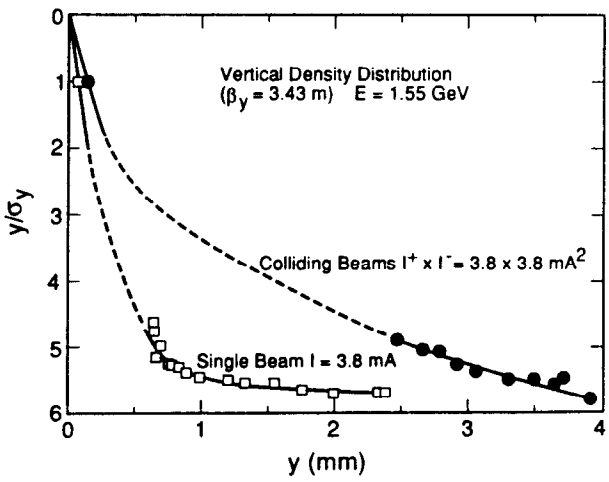

FIG. 2. Particle distributions measured in SPEAR with and without the beam-beam interaction using a scraper [2].

Even neglecting the effect of the scraper on beam, still the density profile is not measured directly by the scraper measurements and must be inferred. The argument used for this inference is given in an appendix. Our simulations support the inference, indicating departures of 20% between inferred densities and simulated densities (see Figure 11). On the logarithmic scale relevant to this discussion, this is good agreement.

Before beginning our discussion of the theoretical situation, we wish to specify our notation and vocabulary. The linear betatron motion around the ring is given by the standard Floquet solution,

* This work was performed while the author was a visitor at the Wilson Laboratory, Cornell University, Ithaca, NY 14850. Address after July 1, 1989 is SLAC, Stanford, CA 94305.

† Operated by Universities Research Association, Inc., under contract with the U.S. Department of Energy.

Contributed to the 3rd Advanced ICFA Beam Dynamics Workshop:
Beam-Beam Effects in Circular Colliders, Novosibirsk, USSR, May 29–June 2, 1989

$$x(s) = \sqrt{2J_x\beta_x}\,\cos(\theta_x + \phi_x(s))$$

$$y(s) = \sqrt{2J_y\beta_y}\,\cos(\theta_y + \phi_y(s)), \qquad (1)$$

where J_x and θ_x are the action and angle variables respectively for the horizontal x betatron motion. We introduce the amplitudes A_x and A_y

$$A_x = \sqrt{2J_x} \qquad A_y = \sqrt{2J_y}, \qquad (2)$$

and, since the bulk of the particles are in a well defined bi-Gaussian core it is convenient to measure amplitudes in terms of this core size by introducing normalized amplitudes a_x and a_y.

$$a_x = A_x/\sigma_{A_x} \qquad a_y = A_y/\sigma_{A_y}. \qquad (3)$$

Similarly, the longitudinal synchrotron motion may be parameterized as

$$c\tau = a_e\,\sigma_{c\tau}\,\sin\theta_e$$

$$\frac{\delta E}{E} = a_e\sigma_e\,\cos\theta_e. \qquad (4)$$

Here a_e is the normalized energy amplitude. $\sigma_{c\tau}$ is related to σ_e through the RF parameters and the momentum compaction.

The actions (or amplitudes) are the appropriate variables to study, since they change only very slowly as a result of the nonlinear forces and/or quantum excitation.

No analytical calculations of tail distributions are known to us. Even simulations are unavailable. The reason for the lack of simulations can be quite readily appreciated. Suppose that one were tracking an ensemble of N particles, observing the flow of particles across a boundary. The expected number ΔN that will cross the boundary in time Δt is approximately

$$\Delta N \approx dN/dt \cdot \Delta t = -\frac{N}{\tau_s} \cdot \Delta t, \qquad (5)$$

where τ_s is the lifetime associated with a scraper at that position. The number passing in n turns is found by setting $\Delta t = nT$ where T is the orbit period, about 2.6 microseconds for CESR. To achieve a $\Delta N = 30$, for a statistical uncertainty of 20% in ΔN, lifetimes of 12 minutes to 2 hours would require a product nN equal 10^{10} to 10^{11} particle-turns. 10^8 particle-turns per cpu hour has been achieved on supercomputers using streamlined codes [5]. Thus modeling tails out to these lifetimes would require 100 to 1000 hours of supercomputer time. One needs to reduce these times by a factor of several hundred if simulations are to be a useful design tool.

Our idea is to take advantage of the slowly varying statistical nature of the changes in amplitude. One may verify that the change in any of the three normalized amplitudes on a single turn due to quantum excitation is the order of 1%. The change of the betatron amplitudes from a single beam-beam kick is less than 5%, with a few turn average equal to 0.05 divided by the number of turns. Macroscopic changes in particle distributions require a damping time which is 10,000 turns for CESR. Thus a particle at 6 to 10σ in the vertical tails does not suddenly hop there from the core, but must proceed there slowly, undergoing many beam-beam kicks and quantum excitations and dampings in the process. It follows that for a particle in the tail the exact knowledge of its history in the core is lost and irrelevant. One could replace the exact core by statistical information of core behavior.

Rather than tediously tracking billions of particle-turns in the core to get information about tail particles, we propose to track core particles for a damping time (after the core has settled) gathering information we can use later. We do this by drawing an imaginary boundary in normalized amplitude space at a radius where out of the 1000 particles we are tracking, about 100 particles typically lie outside this radius and the remaining 900 lie inside (see Figure 3). At each turn we determine if a particle is inside or outside of this boundary. If it has moved upward across this boundary we save its new coordinates (say in file #1). We do this for a damping time of 10,000 turns, saving all such "coordinates of arrival", and additionally every ten turns, we randomly select one of the particles in the outer region and save its coordinates in a separate file (#3).

Next we proceed to step 2. We distribute the 1000 particles according to the coordinates saved in file #3, and begin to track these particles. We again draw a boundary so that about 100 particles are outside it. If, as we track, a particle falls downward across the lower boundary we choose a coordinate set at random from file #1 created in step 1, and "reinsert" this particle above the lower boundary for further tracking. We track in this way for a damping time. Then we begin to save coordinates of particles crossing the upper boundary and put them into a file #2. Similarly every 10 turns we pick a particle at random which is outside the upper boundary and save its coordinates in file #3.

Step 3 is identical to step 2. In step 4 (or the last step) there is no upper boundary. After a damping time we begin to save coordinate positions of particles in the tail.

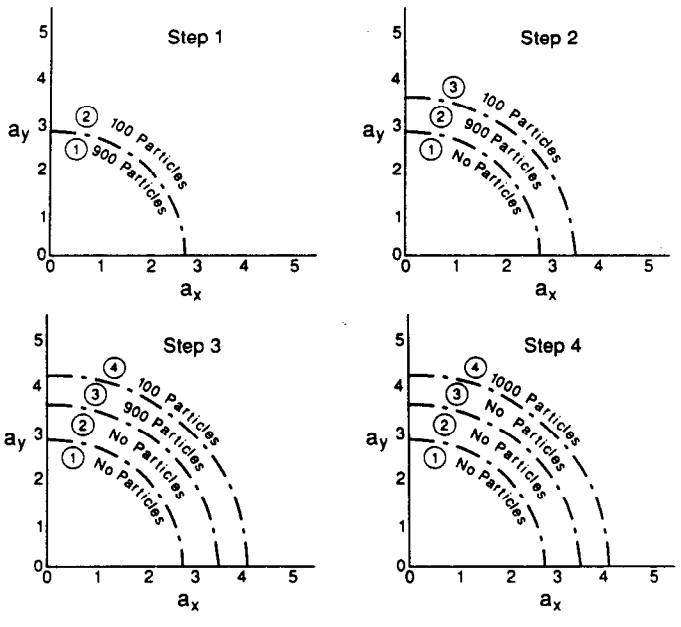

FIG. 3. Typical amplitude space boundaries. At each step final coordinates of outward transversals at upper boundary are saved to use for re-injection of inward transversals at that boundary in subsequent step.

At each step we gain a factor of 10 for the number of particles in the tail. In step 4 we have 1000 particles in a region where there was only one particle in step 1. To get this information we have had to track: i) 2 damping times to find the self consistent core size (see below), ii) 1 damping time in step 1 to gather information, and iii) 1 damping time for settling and 1 damping time to gather information in steps 2, 3 and 4. This is a total of 9 damping times, 7 after the core size is determined. If we had attempted to get the same information tracking an ensemble of 1,000,000 particles, we would have needed to track that ensemble for 2 damping times. The net reduction in cpu time using the strategy outlined is thus about a factor of 300.

The Model

The computer code we used for tracking particles was a minor enhancement of a code created by Gerry Jackson [5]. Jackson wrote a code to simulate core behavior under beam-beam operating conditions, including all relevant physics and omitting the irrelevant, with the objective of generating a fast code that could track a statistical ensemble of particles for several damping times. He achieved a code that tracks 10^8 particle-turns per cpu hour on a Floating Point Systems array processor attached to the Cornell IBM 3090 supercomputer. A vector multiplication call takes about 0.5 microseconds per multiplication. Jackson tracks a half turn (one IP and one arc) with the time equivalent of 36 multiplications. His code includes:

- two beam-beam interaction points,
- linear transport through the arc with an energy dependent phase advance and beta functions,
- rf acceleration and quantum excitation in one arc,
- a beam-beam kick derived from the error function solution for the field of a bi-Gaussian charge distribution of a fixed (self-consistent) counter-rotating beam,
- the vertical height of the bi-Gaussian distribution taken to depend on the arrival time of the tracked particle (see Figure 4).

The arc transfer matrices are calculated and stored for a discrete set of energies, centers of energy bins. At execution time the energy bin is determined and the appropriate transfer matrix used.

The beam-beam kick is pre-calculated for a three dimensional grid of points with coordinates $(x/\sigma_x, y/\sigma_y, \sigma_x/\sigma_y)$. A ten-point interpolation determines the kick at execution time.

Not included are:

- effects of sextupoles other than the energy dependent tune modulation,
- coupling, and
- machine-beam coherent effects.

Coupling is simulated by adding a small amount of vertical quantum excitation.

Different settings of sextupoles even with the same chromaticity can dramatically affect beam lifetime. However for the usual sextupole settings, the field strengths are very small near the beam core. This has led us to posit the situation depicted in Figure 5. The tail is supposed to consist of three regions. In the inner region, which we call the near tail, the sextupoles are still negligible. Beam-beam dynamics are determining the shape of the tail. In the middle region, the intermediate tail, sextupole

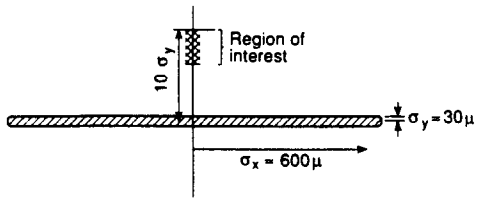

FIG. 4a. The beam cross section at the CESR interaction point.

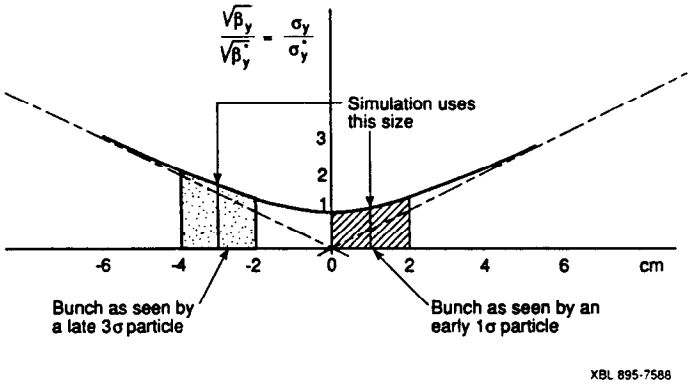

FIG. 4b. The vertical height of the beam as a function of distance from the interaction point. The beam-beam kick depends on the arrival time of the particle. Our algorithm for the kick is based on a 2-D bi-Gaussian distribution of height equal to the height at the center of the counter-rotating bunch.

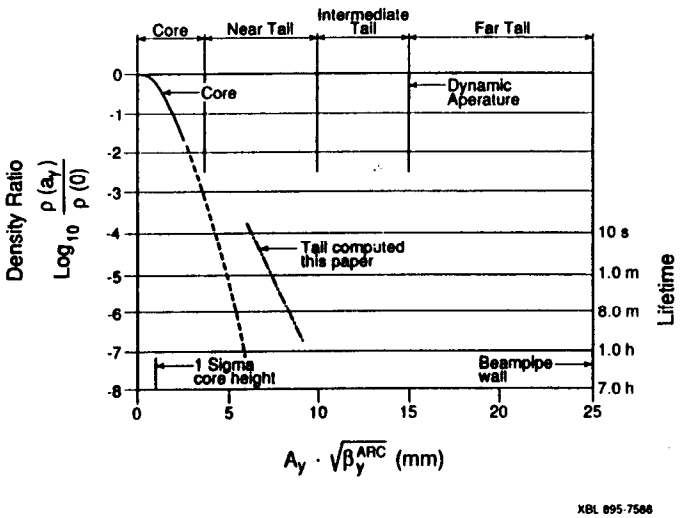

FIG. 5. Vertical particle distribution and corresponding lifetimes from scraper measurements.

effects are important. In the far tail region, particles are swept to the walls in a few hundred turns. In the final section we propose ways to include the sextupoles and extend tail distribution studies into the intermediate region. The present work is limited to the near tail region.

Core Distributions

The computer code of G. Jackson is able to predict CESR core sizes to within 15%. We have appended subroutines associated with storing and selecting particle coordinates at the amplitude

boundaries depicted in Figure 3. Although Jackson has studied interactional dynamics between two counter-rotating beams, we used a version which assumes that one beam is bi-Gaussian of fixed size and the other beam is tracked under the influence of the fixed beam. This is the so called weak-strong beam-beam simulation. We first studied the convergence of the distribution of the tracked (weak) beam.

In Figure 6 we show the behavior of the variance (σ^2) of the vertical amplitude of the tracked beam, beginning with 1000 particles distributed in a Gaussian shape of guessed width. As can be seen from Figure 6, the variance converges in about two damping times, a total of 20,000 turns. Figure 7 shows that the distribution also converges, and in about the same number of turns. Note that if the final distribution were Gaussian, the distribution would be a straight line on this plot. The plot is quite straight when the fixed beam diameter coincides with the final diameter of the tracked beam. For the case shown, the fixed beam has a diameter smaller than the final diameter of the tracked beam.

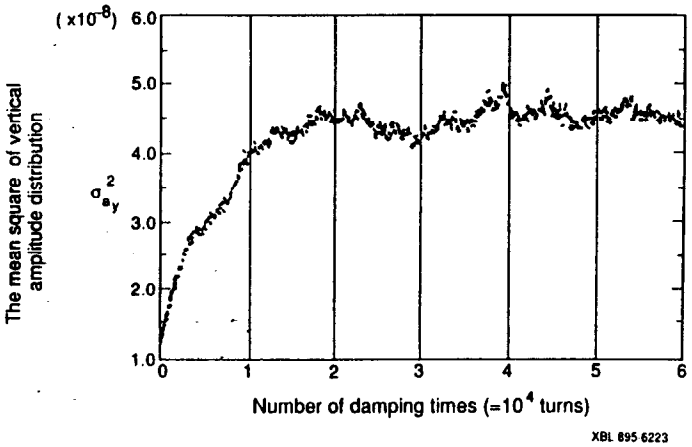

FIG. 6. The σ^2 of the tracked distribution settles nicely in about two damping times. This ambulation of the asymptote is expected for a sample containing 1000 particles.

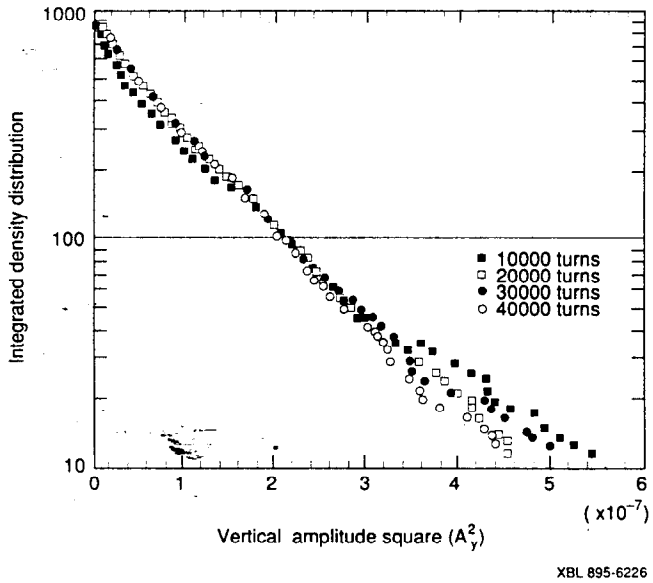

FIG. 7. The integrated (from abscissa to infinity) vertical amplitude distribution of the tracked beam after each of 4 damping times.

Our first task is to efficiently determine the self-consistent diameter. One could track a beam for many fixed beam diameters, and determine the curve of Figure 8. The desired self-consistent diameter is the point at which this curve crosses the diagonal. This point is stable against flip-flop if the angle $\theta < 45°$. It is possible to determine this self-consistent diameter in about 2 damping times by:

i) starting from a guess (point 1 in Figure 8), track for one damping time,

ii) after one damping time (point 2) reset the fixed beam size to this diameter, and

iii) continue to track (point 3).

After a second damping time we have a diameter very close to the desired self consistent diameter.

Tail Distributions

Having found the self-consistent core size, we begin to save coordinates as particles cross the boundary we have drawn in step 1, Figure 3. Then we proceed through the steps 2, 3, and 4 outlined in this Figure, and described in the introduction above. We now present some results (Figures 9–14) obtained for CESR operating conditions. See Table 1.

Figure 9 shows the vertical density profile obtained for particles between 6 and 10σ from the beam core. It is remarkably exponential except for the tip of the tail where, because of poor statistics, exact numbers are not meaningful.

During step 4, we also kept track of the maximum amplitude achieved by each particle. With this information we can determine lifetime for any amplitude, since particles with maximum amplitude larger than that amplitude would have hit the scraper. A graph of lifetime versus amplitude is shown in Figure 10. Note that lifetimes correspond to a range that can be measured experimentally.

From these lifetimes we can infer particle densities using the arguments presented in the appendix. The resulting inferred density, together with the correct simulated density, are shown in Figure 11. Remarkably the two curves are parallel to one another and separated by a constant factor of 0.8. Inferred distributions are apparently quite reliable.

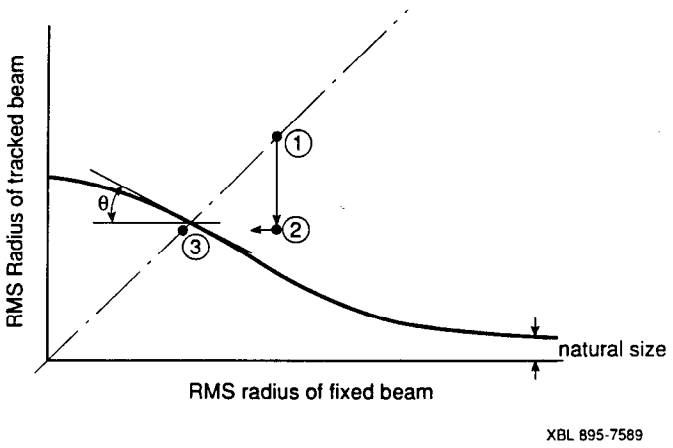

FIG. 8. The rms radius of the tracked beam as a function of the radius of the fixed beam. Assuming point 1 was the first guess for the tracked beam, then after 1 damping time the height will have decreased to point 2. The fixed beam size is now changed to point 3, and tracking continued for another damping time. Convergence to the diagonal crossover is very rapid.

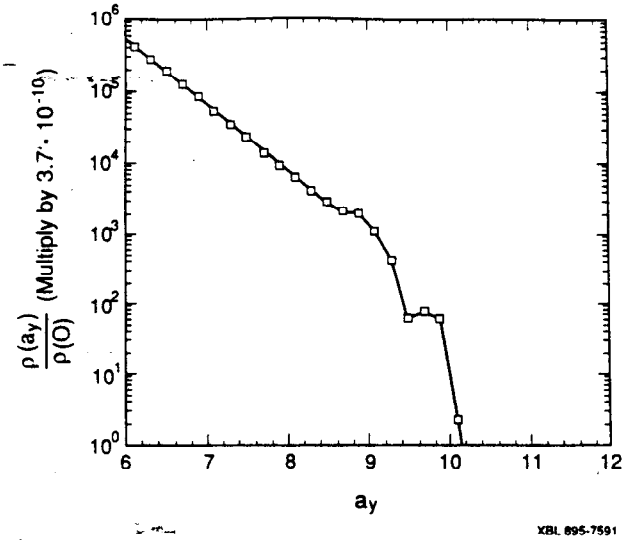

FIG. 9. Density vs. vertical amplitude beyond 6σ. It is very close to exponential except at the outer edge where statistics are poor.

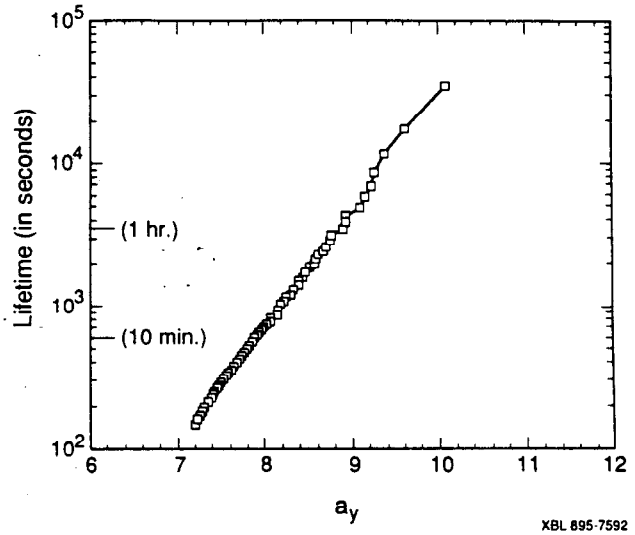

FIG. 10. Beam lifetimes that would result from a scrapers placed at the amplitude of the abscissa.

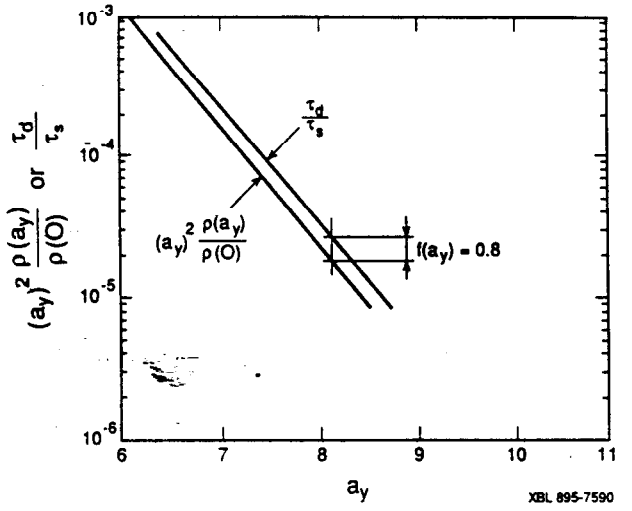

FIG. 11. Comparison of particle density profiles that would have been inferred from lifetime measurements with the actual simulated distribution.

Table 1. CESR Operating Parameters (June 1987).

Orbit Period (T)		2.56×10^{-6} sec
Energy		5.29 GeV
Energy Spread		6×10^{-4}
Energy Loss/Turn		1.03 MeV
Bunch Length ($\sigma_{c\tau}$)		2.2 mm
Betatron Damping Time (τ_d)		25 ms
Beam Current		8 ma
Momentum Compaction		0.0154
Beta Function at IP's	H	1.05 m
	V	0.02 m
Eta Function at IP's	H	0.68 m
	V	0
Beam Size at IP (σ_x or σ_y)	H	0.60 mm
	V	0.03 mm
Phase Advance/Turn	H	29.498 cycles
	V	29.430 cycles
Chromaticity	H	0.5
	V	0.3
Emittance	H	0.16 mm·mrad
	V	0.04 mm·mrad

The next two Figures, 12 and 13, are cuts through the distribution data displayed in Figure 9. Figure 12 shows the contribution to the vertical density distribution from particles in fixed horizontal amplitude bins. Figure 13 shows the contributions to this distribution from particles in fixed energy amplitude bins. The circled ratios on the graphs indicate the relative fraction of particles in the core that populate that particular amplitude bin. These graphs demonstrate that particles in the vertical tails tend to have large horizontal amplitude and large energy amplitude.

In addition to bin populations, we also saved information on crossings of bin boundaries. From this data we extract information on particle motion. An example of information of this type is shown in Figure 14. Here we show the vertical flux as a function of horizontal and vertical amplitude. Positive values indicate outward vertical flux. We see that particles tend to move outward into the vertical tail at large horizontal amplitude and fall back into the core at small horizontal amplitude. Of course, particles damp from large horizontal amplitude toward smaller horizontal amplitude, so one is seeing a circulation pattern. Particles that wander statistically into the horizontal tails experience a region of strong non-linearity, get pushed up into the vertical tails. From there they damp toward smaller horizontal amplitudes and then fall back into the core. Many plots of this nature can be constructed to study the dynamical structure of tail distributions.

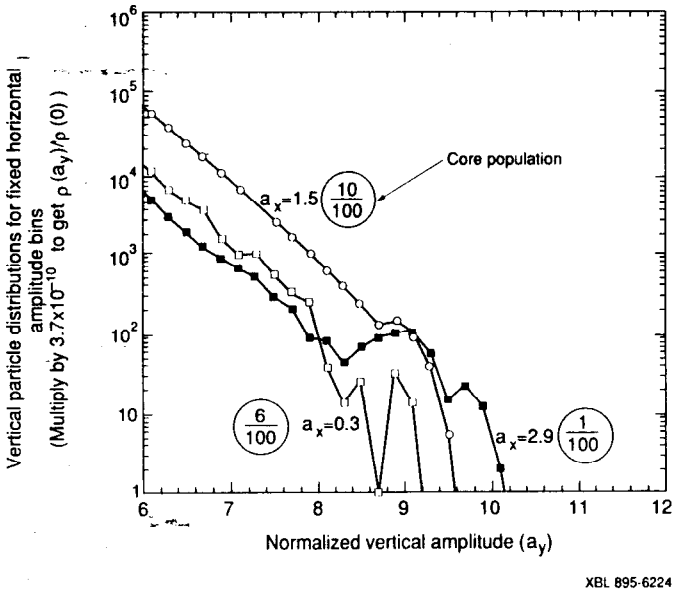

FIG. 12. Vertical particle distributions for fixed horizontal amplitude bins showing that particles with large horizontal amplitude are more prevalent in the vertical tail.

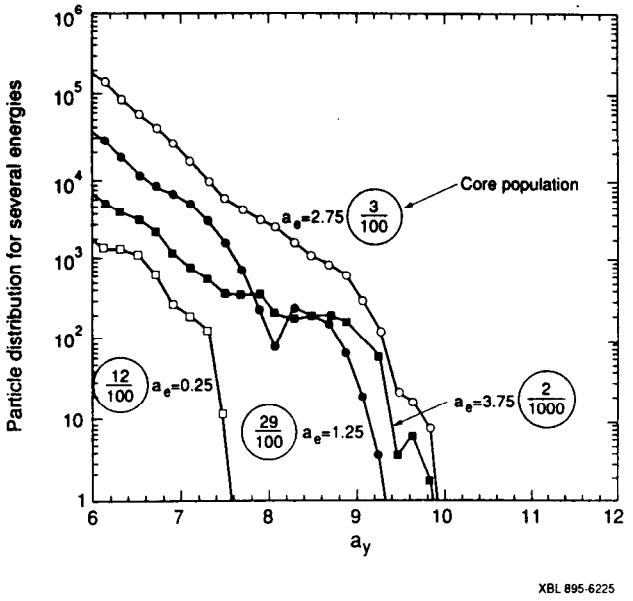

FIG. 13. Vertical particle distributions for fixed energy amplitude bins showing that particles with large energy amplitudes are more prevalent in the vertical tail.

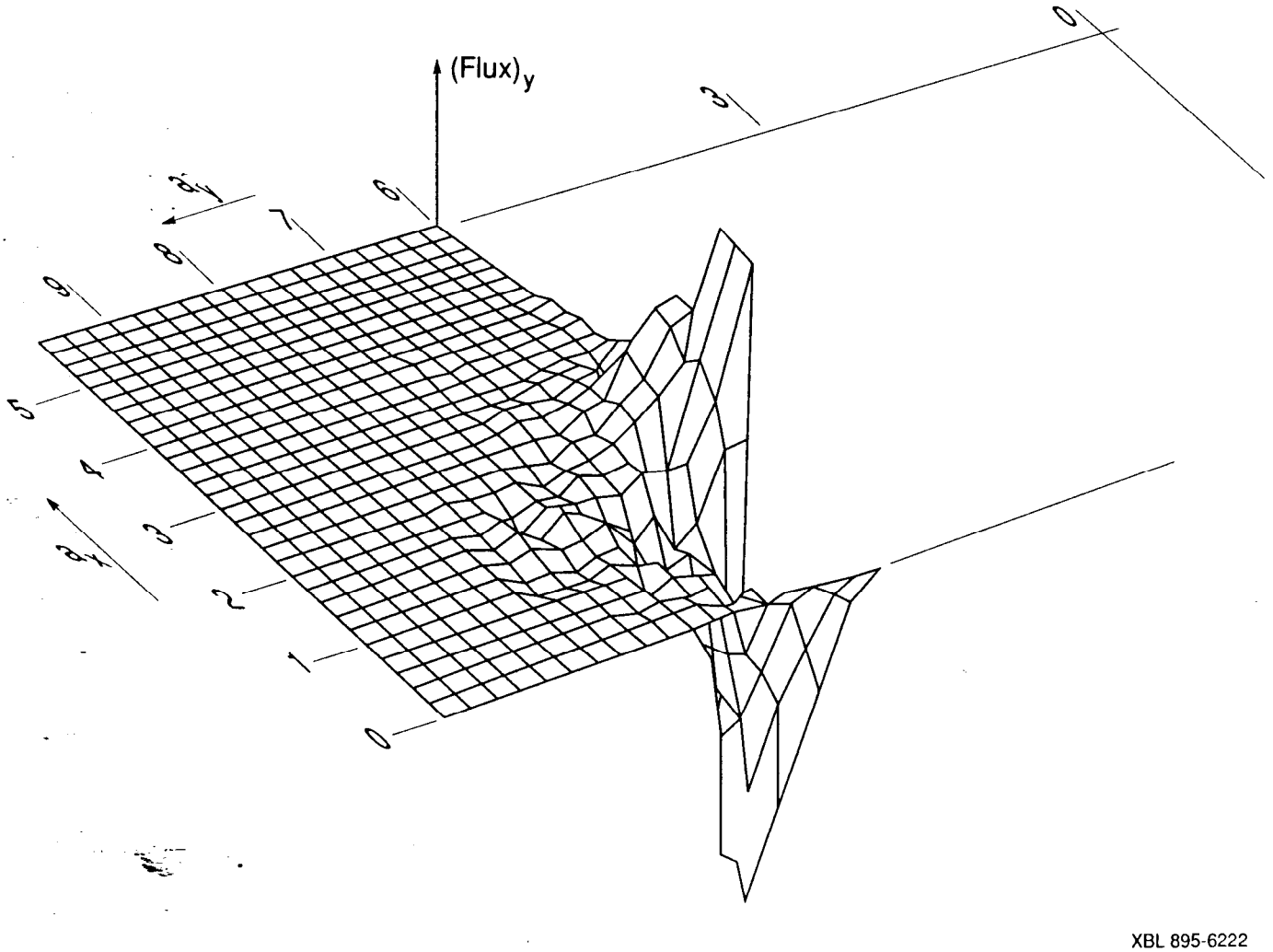

FIG. 14. A profile of particle flux in the vertical direction showing a circulation pattern in the vertical tails. Particles move outward at large horizontal amplitudes and fall back into the core at small horizontal amplitudes.

Discussion

It may appear at first sight that correlations between where a particle moves downward and later upward across an amplitude boundary would invalidate the method we are proposing. However, particle identities are interchangeable, and it is entirely appropriate to have a statistical response to the event "crossing the boundary."

However, there are two conditions that must be satisfied for our method to be valid. The first condition requires there be no rare, but important, crossings of a lower boundary which lead with high probability, to a crossing of the upper boundary. Secondly the distance between subsequent boundaries must be large enough so that the exact position where a particle crossed the lower boundary has been forgotten by the time it crosses the upward boundary. Since it is expected that transport from one boundary to the next involves hundreds of turns, especially if the first condition is satisfied, then the magnitude of the quantum excitation is such that indeed the beginning position gets lost.

It is our opinion that a rare, but important, event will not occur as a result of arriving at special betatron angles. However a high energy particle in the core could be rare and important since high energies clearly feed the tails. This situation must be looked at quantitatively by tracking the "inner" segment ten damping times, comparing the results with tracking the "upper" segment one damping time. Unfortunately the author's visit at Cornell came to a close before these comparisons could be investigated.

A discrepancy arising from rare higher energy particles could be overcome by introducing boundaries in the three-dimensional amplitude space, as shown in Figure 15. It is assumed that the boundaries are invariant under rotation in the (a_x, a_y) space, although other choices could be made. Here

$$a_r = \sqrt{a_x^2 + a_y^2}\,.$$

In order to include sextupole effects, we suggest a kick factorization of the one turn map. The amplitudes are small enough that such a factorization should be well behaved. This form of tracking will only be necessary in the tails, and should be fast enough to achieve acceptable computation times.

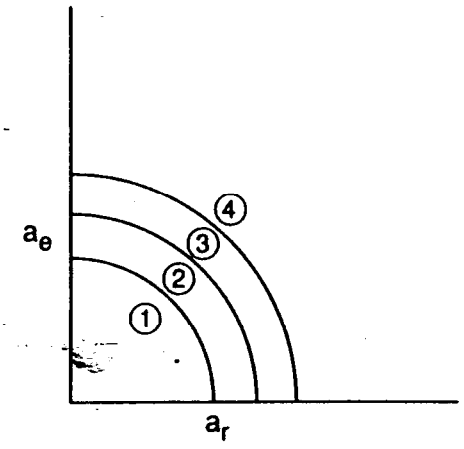

FIG. 15. Rare motion to large energy amplitudes in the core region may give a contribution to the vertical tail population that we have overlooked. Three-dimensional boundaries would be required to detect this motion.

Finally, though we believe that the methods we have described, or a modification of them, will enable determination of tail particle distributions, it will be important in any application of the method to include some long runs to numerically affirm the validity of the process.

Appendix: Inferring Tail Distributions from Scraper Measurements

To infer the particle density distribution one posits a model in which the outward flow into the tail occurs in a separate part of the phase space from the inward flow, and that the inward flow occurs primarily as a result of damping. Specifically one supposes that is possible to distinguish outward moving particles from inward moving particles, such that the total density of particles at any instant at vertical amplitude A_y would be given by

$$\rho(A_y) = \rho_o(A_y) + \rho_i(A_y) \qquad (A1)$$

and, assuming the scraper is withdrawn from the beam and the lifetime very long, the flux balance equation at A_y would be given by

$$F^\infty(A_y) = F_o^\infty(A_y) - F_i^\infty(A_y) = 0 \qquad (A2)$$

If the particles that were moving inward were doing so as a result of damping, then

$$\frac{dA_y}{dt} = -\frac{A_y}{\tau_d} \qquad (A3)$$

where τ_d is the betatron damping time. Thus the inward flux would be just

$$F_d(A_y) = \frac{2\pi A_y \rho_i(A_y) dA_y}{dt} = \frac{2\pi A_y^2 \rho_i(A_y)}{\tau_d} \qquad (A4)$$

If a scraper were inserted at amplitude A_y the flux at the scraper would be given by

$$F_o^s(A_y) = -\frac{dN}{dt} = \frac{N}{\tau_s} \approx \frac{2\pi\rho(0)\sigma_{A_y}^2}{\tau_s}$$

where τ_s is the measured lifetime with the scraper in place. The above approximation is very accurate since the vast majority of the particles are in the core. We may now write the following set of inequalities.

$$F_o^s(A_y) \le F_o^\infty(A_y) = F_i^\infty(A_y) \le F_d(A_y)$$

$$F_d(A_y) = \frac{2\pi A_y^2 \rho_i(A_y)}{\tau_d} \le \frac{2\pi A_y^2 \rho(A_y)}{\tau_d}\,. \qquad (A6)$$

The first inequality follows from the fact that the inward flow would be expected to feed the upward flow to some extent. With the inward flux removed, the outward flux would be reduced. The second inequality follows from the fact that the beam-beam scattering will inhibit the inward flow of particles. The remaining equality and inequality follow from Equations (A2) and (A3). Hence

$$\left(\frac{\tau_d}{\tau_s}\right) = f(A_y)\left(\frac{A_y}{\sigma_{A_y}}\right)^2 \frac{\rho(A_y)}{\rho(0)}\,, \qquad (A7)$$

where we are guaranteed by Equations (A6) that $f(A_y) \leq 1$. To infer particle densities from lifetime measurements it is assumed that $f \approx 1$. Our simulations have $f \approx 0.8$, so apparently this inference is adequate to yield a qualitative picture. Also the flux simulation illustrated in Figure 14 appears to validate the two flow model assumed here.

Acknowledgements

The author wishes to sincerely thank R. Siemann for inviting him to Cornell and suggesting this problem, G. Jackson for supplying the computer code and answering a host of questions, Raphael Littauer for overseeing this work and providing many insights into storage ring physics, and to Steve Milton for many detailed discussions, computer support, and help with the basics of the beam-beam interaction.

References

1. G. Decker and R. Talman, *IEEE Trans. Nucl. Sci.* NS-30, No. 4 (1983), p. 2188.
2. H. Wiedemann, AIP Conference on Nonlinear Dynamics and the Beam-Beam Interaction, Brookhaven, 1979, p. 84.
3. S. Myers, Review of Beam-Beam Simulations, Nonlinear Dynamics Aspects of Particle Accelerators, Sardinia, 1985, p. 176.
4. S. Milton and R. Littauer, "Measurement and Simulation of Beam-Beam Effects in the Weak/Strong Regime," *Bull. of the APS, 34,* No. 2 (1989), p. 221, and S. Milton, Cornell University, Ph.D. thesis (1989).
5. G. Jackson, "The Theory, Simulation, and Measurement of the Cornell Electron Storage Ring Luminosity Performance," Cornell University, Ph.D. thesis (1987).